Senescence and Spectral Reflectance in Leaves of Northern Pin Oak (*Quercus palustris* Muenchh.)

M. BOYER,* J. MILLER,† M. BELANGER,* and E. HARE‡

York University, North York, Ontario, Canada M3J 1P3

JIYOU WU

Department of Optics, Shandong University, People's Republic of China

Changes in the anatomy of oak leaves and their reflectance spectra from 450 to 850 nm were followed during autumnal senescence. Six sequential stages of senescence identified from green healthy to bronze dying leaves, and their reflectance properties are described. Changes in leaves related to the senescent stages, and factors exerting the most significant effects on reflectance, included the decline in chlorophyll, the synthesis of anthocyanins, the dissolution of organelles, and the dessication of tissues. Randomly collected leaves from sample trees were subsequently classified visually and examined for specific spectral features of the "red edge" as identified by Horler et al. (1983), Hare et al. (1984a,b), and Miller et al. (1985). The Gaussian model of the red edge, described by Hare et al. (1984a,b) and Miller et al. (1985), provided a reliable way of identifying the senescent classes. When compared with the non-Gaussian reflectance features by means of a discriminant function analysis, the latter proved to be less reliable.

Introduction

The changes characteristic of fall senescence in leaves of forest trees in temperate regions have been investigated by many workers (for reviews, see: Verner, 1961; Thomas and Stoddart, 1980; Thimann, 1980; Woolhouse and Jenkins, 1983). It is clear that the processes involved are programmed genetically through a sequence of metabolic and structural changes ultimately leading to abscission and death. Among the more striking events in temperate zones particularly is the development or unmasking of colored pigments: anthocyanins, carotenoids, and xanthophylls, which usually follow a decline in chlorophyll (Goodwin, 1958; Moore, 1965; Sanger, 1971).

These and less visually striking processes have obvious relevance to geobotany, particularly the detection of mineral stress in plants through remote sensing (Goetz et al., 1983). Not only does it seem logical that many of the processes described are operative in mineral-induced senescence, but observations of premature fall senescence syndromes have already been reported by Canney et al. (1979), Labovitz et al. (1985), and Schwaller and Tkach (1980; 1985) on mineral-stressed sites.

Foliar senescence produces significant spectral fluctuations in three regions of the electromagnetic spectrum between 450 and 2500 nm: 1) between 450 and 750 nm, in which changes in chlorophyll in particular, but other pigments as well, play a major role; 2) between 750 and 1400 nm, in which the internal cellular

*Department of Biology.
†Department of Physics and Centre for Research in Experimental Space Science.
‡Centre for Research in Experimental Space Science.

52 Vanderbilt Ave., New York, NY 10017 0034-4257/88/$3.50

geometry of the leaf is dominant; and 3) between 1400 and 2500 nm, where leaf water content is important. Whereas a role for all of these regions may be inferred from the literature, of particular interest is the red shoulder or edge between 700 and 750 nm (Collins et al., 1983; Hare et al., 1984a, b; Horler et al., 1983; Miller et al., 1985). This steep reflectance edge has been observed to shift towards longer (red shifts) or shorter (blue shifts) wavelengths, these being considered indicators of mineral stress.

Hare et al. (1984a,b) and Miller et al. (1985) have extended the usefulness of this spectral region in geobotanical work through the introduction of an inverted Gaussian model to describe the red edge. Three red edge Gaussian model parameters, i.e., the shoulder reflection (R_{sg}), chlorophyll-well reflectance minimum (R_{0g}), and the inflection wavelength (λ_{pg}) have proved useful in the detection of senescence.

In this study, anatomical and physiological observations on the senescing leaves of pin oak, when carried out in conjunction with ground-based reflectance analyses, provide further substantiation for the validity of the red shoulder, its Gaussian model representation, and the visible light spectrum as indices of senescence.

Methods

Data presented here were obtained from a row of norther pin oaks (*Quercus palustris* Muenchh.) located on the esplanade of the administrative building at York University, North York, Ontario. The trees (Fig. 8) were of uniform age ($\pm$25 years) and were of horticultural origin. They were planted in deep concrete wells and artificially watered. Although generally in good condition, several specimens suffered from chronic iron-deficiency chlorosis, as noted (Treshow, 1970). The trees exhibit fall coloration patterns reminiscent of scarlet oak (*Quercus coccinea* Muenchh.), for which they are sometimes mistaken. Visual symptoms of senescence on these trees have remained relatively constant through the years, but time of initiation, the duration, and the intensity of symptoms have varied widely seasonally and among trees at any one season. Observation of individuals over 2 years with respect to these parameters appears to be consistent and may reflect genetic differences among them.

Ten trees were selected for more intensive observations through the period from 5 September to 9 October, 1985. Written and photographic records of trees were maintained for reference. For color records, Kodak High Speed Ektochrome and High Speed Infrared film were used, the latter with a Wratten #25 filter. Visually significant stages in the progression through fall senescence in pin oak were assigned the following acronyms:

- G for green leaves without other visible coloration.
- G_c for green chlorotic leaves without red coloration.
- S_{early} for scarlet leaves with color dominated by chlorophylls and anthocyanin pigments but with reduced chlorophyll content when compared with G leaves.
- S_{late} for scarlet leaves with color dominated by anthocyanins but with much reduced chlorophylls.

R for red leaves dominated by anthocyanins and carotenoids.

B for bronze leaves exhibiting early stages of the bronzing associated with tannin formation.

Yellow leaves were not considered to be part of the normal syndrome of healthy trees but were sometimes common on leaves from trees with iron-deficiency symptoms which failed to develop typical striking color patterns.

Both spectral and anatomical studies were performed jointly on individual leaves of G, G_c, S_{early}, R, and B categories. Following spectral analysis as described below, the "mirror image" side of the target area showing clear symptoms was excised and fixed in FAA (Sass, 1951). The segment removed was approximately 4×8 mm and was cut parallel to the long axis of the midrib near the base. Following fixation, tissues were dehydrated in TBA embedded in paraplast and sectioned at 5nm with a rotary microtome. Staining was in safranin, fast-green (Sass, 1951).

The study of the corresponding spectral properties involved laboratory reflectance measurements of excised leaves, using a Jobin Yvon Optical System Model H_2O V-IR grating spectrometer, which were scanned 450–850 nm at a spectral resolution 4 nm. For each of the 10 trees under investigation, leaves were collected in stacks of 10 leaves and placed in custom-designed sample holder that permits the spectrometer to view either the leaf stack or a $BaSO_4$ standard reflectance surface along the surface normal. The leaf stack was positioned in the sample holder so that the field of view of the spectrometer observed a 1 cm^2 area to one side of the leaf midrib near the widest part of the leaf. The analog signal from an Alphametrics Model DC 1010 radiometer with a silicon detector is digitized for each of the two scans and stored on a microcomputer, permitting a subsequent calculation of the spectral reflectance as a simple ratio of the signals at each wavelength. The illumination source, a 100-W tungsten-halogen lamp, was collimated and directed at the target at a fixed incidence angle of approximately 20°. Thus these data provide a measurement of the spectral reflectance, or more specifically, the bidirectional reflectance at incidence angle 20° and normal viewing (Swain and Davis, 1978).

In addition to visual inspection of the spectral reflectance curves, subsequent quantitative spectral analysis of these data focussed on the red edge spectral range (670–800 nm). In this analysis, the inverted Gaussian model for the vegetation red edge reflectance (Hare et al., 1984a, b; Miller et al., 1985) was fitted to each spectrum to obtain the red edge parameters mentioned previously. These parameters permit a quantitative description of reflectance changes in the red edge spectral region.

Features of the spectral reflectance curves utilized for descriptive or statistical purposes included the following: 1) from the Gaussian model of the red edge (Hare et al., 1984a, b; Miller et al., 1985), R_{sg} (the Gaussian shoulder reflectance), R_{0g} (the Gaussian reflectance minimum), and λ_{pg} (the Gaussian inflection point) and 2) from the unmodified data R_s and R_0, the shoulder reflectance and the red edge minimum reflectance, respectively, λ_0 (the wavelength corresponding to R_0), λ_{pr} (the red edge inflection point), and σ (the curve width parameter). For descriptive purposes λ_{560} (the chlorophyll reflec-

tance maximum), λ_{450} (the short wavelength absorption shoulder), and λ_{650} (designated the anthocyanin reflectance maximum) were useful. Parameters of the red shoulder taken from samples classified as to senescent type by both visual and spectral analyses into senescent categories were later subjected to a discriminant function analysis as outlined by the SAS Institute (1985). This discriminate procedure assumes a prior knowledge of the classes to be differentiated (i.e., senescent stages) and computes a quadratic discriminate function based on the numeric parameters. In previous applications cited in the reference, the discriminate function was applied to classifying agricultural crops from data collected by remote sensing.

Results

Many of the structural features, and by inference, physiological changes, in leaves were tabulated in this study. Fully turgid leaves of pin oak have a compactly arranged bifacial structure (Figs. 1–7). The adaxial (upper) surface consists of two layers of palisade cells, the upper densely and uniformly packed, the lower shorter and in looser array. The abaxial (lower) surface consists of parenchymatous cells relatively irregularly spaced with a high noncellular volume (the spongy parenchyma). The epidermal system is unistratose, consisting of isodiametric cells with somewhat undulating walls as seen in whole section. Stomata are confined to the lower surface. Appendages are not observed, but a pronounced cuticle is present over both surfaces. The reticulated vein system (Fig. 5) segregates the mesophyll into small islands or areoles ± 1.0 mm in diameter. The larger veins forming their borders are supported by a girder system continuous with the bundle sheath cells (Fig. 5). Smaller veins are suspended in the surrounding parenchyma and often end blindly in the mesophyll. The reduction in chlorophyll, the lack of intercellular

FIGURE 1. Leaf type G_c. Arrows locate starch containing plastids in palisade layer (upper) and spongy parenchyma (lower). Nuclei appear to be positioned centrally in cells. The few chloroplasts and thin leaf are suggestive of iron-induced chlorosis ($\times 550$).

FIGURE 2. Leaf type G. Chloroplasts are located peripherally in the cell. Apparent absence of chloroplasts in upper palisade layer (arrows) is a fixation artifact (×550).

space, and the reduced cell size characteristic of the tissues of the conductive system are in sharp contrast to the mesophyll and probably contribute to a reduction in shoulder reflectance. The visible intracellular features observable either directly or indirectly in tissues processed by the above methods include cytoplasm nuclei, nucleoli, chloroplasts, and vacuoles (Figs. 1–4). Ergastic substances which can be observed include starch (Fig. 1) and tanniferous inclusions (Fig. 6), probably hydrolyzable tannins (Ribereau-Gayon, 1968), and crystals in the bundle sheath cells. Anthocyanins being soluble cannot be directly detected. Chloroplasts in fully turgid cells are pressed against the cell wall (Fig. 2) by

FIGURE 3. Leaf type S_{early}. Degeneration of chloroplasts and other organelles beginning in the upper palisade layer has progressed into the lower palisade layer (arrows) (×550).

FIGURE 4. Leaf type S_{late}. Breakdown of organelles has progressed into the spongy cells. Those nearest the substomatal chamber still retain plastids (arrow) (×550).

the vacuolar membrane (Fig. 2). Nuclei appear sometimes centrally located and at other times peripherally located in the cells with respect to the short axis. In both cases, however, they appear in sharply defined rows in the upper palisade layer (Figs. 1 and 2). In the lower tier and the spongy mesophyll, the arrangement of cells and cell inclusions is not as rigidly organized. Epidermal cells other than guard cells contain no chloroplasts.

Type leaves varied significantly in several structural properties (Table 1) including leaf width. Variation in leaf widths were compensated for, more by

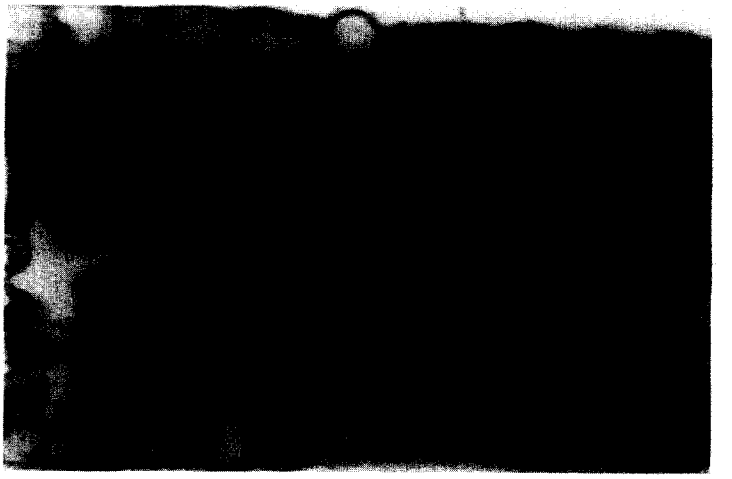

FIGURE 5. Leaf type S_{early} with secondary vein. Clearing has started but chloroplasts are still abundant in the spongy mesophyll. Conductive system remains functional until the leaves dry (×550).

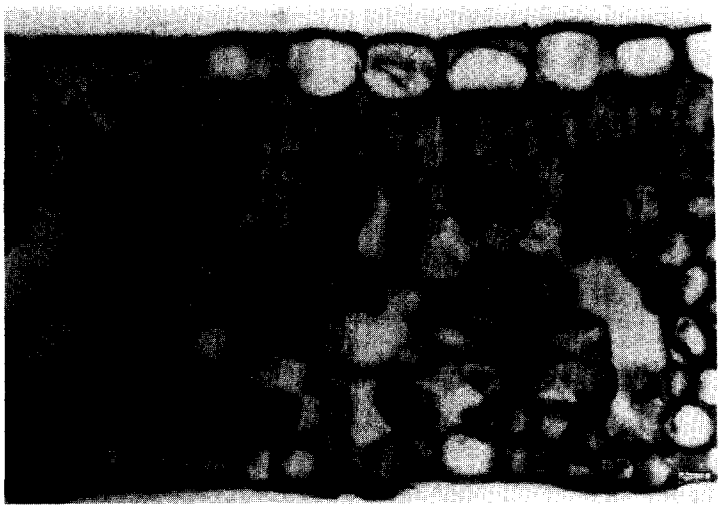

FIGURE 6. Leaf type R. Degeneration of nuclei is progressing leaving cells devoid of visible organelles. Cells still retain their turgidity and conformation (×550).

changes in spongy layer depth than by changes in the palisade layer, which did not differ significantly. Pronounced changes in cell dimensions accompanying increasing senescence were a result of collapse of the cells (Fig. 7, Table 1). The absence of a significant difference in B palisade cell width (Table 1) when compared with G and S_{early} can be attributed to the wide variation among individual cells in the time that they collapse. Minimum cell width recorded in B was 0.7 μm while minimum cell width in G was 5.0 μm.

FIGURE 7. Leaf type B. Precipitated tannins are evident in both the palisade layer and the spongy layer (lower arrow). I beam palisade cells have collapsed. Undulating walls (upper arrows) are indicative of a loss of structural rigidity.

FIGURE 8. *Q. palustris*. Experimental trees 1–8 numbering from zero on the left are illustrated. Trees 1, 2, 5, and 6 are visually S_{early}, and the remainder are G or G_c. Infrared photograph.

Changes in Cellular Characteristics during Senescence

The development of anthocyanin pigments in senescing leaves of healthy plants apparently preceeds the visible loss of chloroplasts (Fig. 9). However, while not discernable visually in S_{early} leaves, gradual loss of chlorophyll appears to begin in most species long before chloroplast degradation is evident (Moore, 1965; Sanger, 1971; Woolhouse and Jenkins, 1983). While these are perceived as the first visible symptoms of the senescence process, they are often followed by a rapid accumulation of anthocyanins and the sequential disappearance of chloroplasts (Figs. 3–7). Water-soluble anthocyanins are not fixed in the process of fixation so that their presence is inferred only from the red coloration of the original specimen.

S state organelle disorganization detected first in the upper palisade layer (the adaxial surface) progresses into the lower palisade layer and hence into the spongy layer (Figs. 3–7). Initially, chloroplast nuclei and the central vacuole retain characteristic forms, particularly in the upper palisade layer (Fig. 2). Gradual displacement and changes in shape of these organelles (Figs. 5 and 6) are an

TABLE 1 Anatomical Measurements of Leaves in Key Stages of Senescence

Acronym	Epidermal Layers Height (μm)	Palisade Layers Height (μm)		Spongy Layer Height (μm)	Cell Dimensions (μm)	
		Total	Upper		Upper Palisade	Spongy Layer
G	14.1 ± 4.4^{a}	66.2 ± 3.6	40.3 ± 2.7	48.5 ± 4.1^{a}	$39.3 \pm 4.1^{a} \times 6.1 \pm 1.3^{a}$	$17.8 \pm 4.9 \times 12.1 \pm 2.0^{a}$
S_{early}	$15.2 \pm 7.3^{a,b}$	68.2 ± 3.3	45.0 ± 3.0^{a}	$58.8 \pm 4.9^{a,b,c}$	$43.7 \pm 4.6^{a} \times 6.8 \pm 0.3^{b}$	$17.7 \pm 3.6^{a} \times 12.4 \pm 2.4^{b}$
R	$13.6 \pm 5.8^{a,b}$	65.6 ± 5.1	$41.9 \pm 3.9^{a,b}$	44.9 ± 11.3^{b}	$41.1 \pm 4.1 \times 3.9 \pm 3.2^{a,b}$	$20.9 \pm 4.7^{b} \times 11.2 \pm 3.4^{c}$
B	14.5 ± 6.1^{b}	67.2 ± 2.7	44.1 ± 3.0^{b}	44.8 ± 4.8^{c}	$43.6 \pm 5.1 \times 5.5 \pm 3.6$	$14.6 \pm 2.6^{a,b} \times 5.1 \pm 3.6^{a,b,c}$

^{a,b,c} Measurements carrying the same superscripts are significantly different from each other, $t = 0.05$. Data are means of 50 measurements selected at random ± 1 SD.

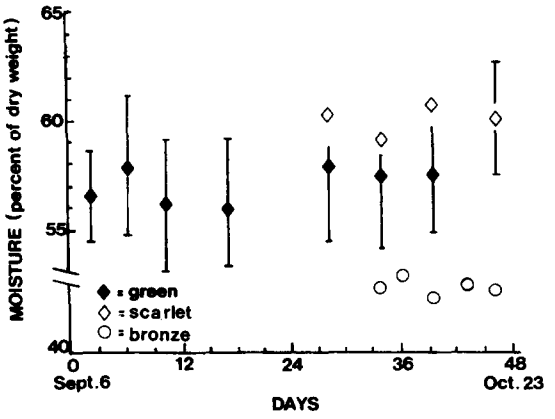

FIGURE 9. Moisture content of leaves of *Q. palustris*. Data with standard deviations are means of at least three samples. Data without vertical bars are representative of individual samples. Sample size was 10 leaves.

integral part of the early senescent syndrome. Dissolution of chloroplasts is completed largely by the S_{late} phase (Fig. 4).

R phase leaves (Figs. 6 and 7) are characterized by the predominance of the carotenoid pigments and anthocyanins and the absence of chlorophyll in keeping with the suggestion that, during the later stages of senescence, chloroplasts and chlorophyll are degraded simultaneously. Nuclear degradation is particularly prominent in R phase leaves (Fig. 6).

In late R and early B phases, tannin like substances accumulate in the vacuoles and are precipitated during the fixation process (Figs. 6 and 7). Later they appear to bind to the cell walls. Until the late R phase the internal geometry of the leaf remains constant (Figs. 6 and 7; Table 1).

Estimates of the moisture content of leaves made periodically through the duration of the field experiment (Fig. 9) clearly support the inference that the leaves drop in moisture concurrent with changes in cell geometry, principally in the late R and B phases. Average cell dimensions, at least along one axis, decline significantly in the late R and B phases (Table 1). This is due principally to the collapse of the lateral walls of the palisade cells (Table 1; Fig. 7), followed later by the collapse of the spongy layers (Table 1).

Tannins accumulated in the early B phase are clearly localized in the vacuoles (Fig. 7), which are probably the last of the organelles to break down (Verner, 1961). Loss of vacuolar membrane integrity is suggested by the deposition of tannins on the cell walls. The latter then stain intensely with the dye safranin following fixation (Fig. 7).

By the late R and B phases the mesophyll of the leaf has collapsed, leaving increased intracellular space (Table 1). Bundle sheath cells and living cells of the vascular strands appear to be functional even after the leaf has dried either on the ground or on the tree.

Changes in Reflectance during Senescence

Comparison of both upper and lower surface spectral reflectances from leaves (Fig. 10) produced spectra similar to those

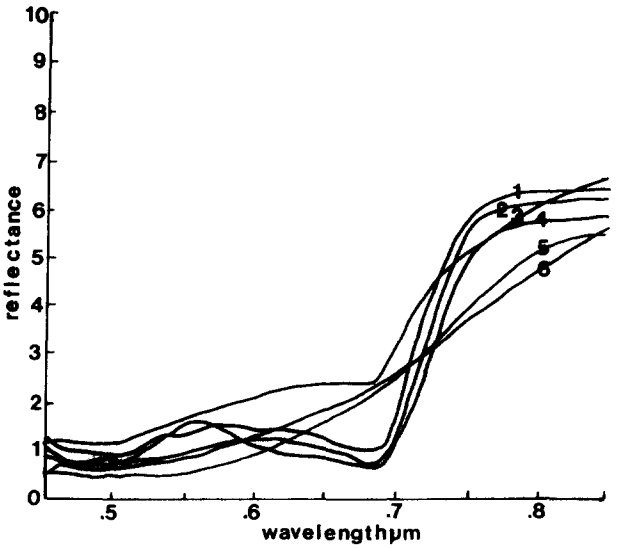

FIGURE 10. Characteristic reflectance spectra from senescing leaves of *Q. palustris* with progressive symtomatological expressions: 1) G_c; 2) S_{early}; 3) S_{late}; 4) G; 5) R; 6) B.

observed in other studies (Billings and Morris, 1951; Gates et al., 1965; Gausman et al., 1967; Knipling, 1969; Moss and Loomis, 1952; Sinclair et al., 1971; Woolley, 1971). G leaves with characteristic anatomy and morphology had discernable reflectance maxima at ±560 nm and reflectance minima at the base of the red shoulder at ±670 nm. The 560 nm shoulder indicates chlorophylls and carotenoid pigments while the ±670 nm minimum locates the second absorption maximum for chlorophylls a and b. The abrupt increase in reflectivity between 700 and 750 nm in the near IR (i.e., the red shoulder) is a manifestation of the transition from the effects of the strong chlorophyll absorption well at 700 nm to dominant light scattering effects of the mesophyll at longer wavelengths (Horler et al., 1983).

The transition from G to S_{late} produces a profound change in the spectral response (Fig. 10). Anthocyanin development dominates the reflectance spectrum. It appears to mask the reflectance shoulder of chlorophyll at ±560 nm (Gausman, 1982), but in turn produces a pronounced reflectance shoulder in the red end of the spectrum at ±650 nm. The apparent stronger absorptance in the region of ±560 nm suggests the possible presence of cyanidine, an anthocyanin absorbing maximally at ±525 nm (Geissman, 1955) and thought to be the major anthocyanin in another species of oak, *Q. ellipsoidalis* E. J. Hill (Sanger, 1971).

The shoulder minimum reflectance (R_0) rises rapidly with the decline in chlorophyll, but the absorption well is usually evident until the late R stage of leaf senescence at which point chlorophylls have largely disappeared from the leaf (Figs. 6 and 10). Shoulder reflectance (R_s) varied with the stage of senescence, but the trend was usually not predictable (Figs. 10 and 11). While moisture content of the foliage declines precipitously only in the B stage (Fig. 9), the strongly absorbing tannins repress the increased R_s usually observed in drying leaves (Allen et al., 1971; Sinclair et al., 1971; Woolley,

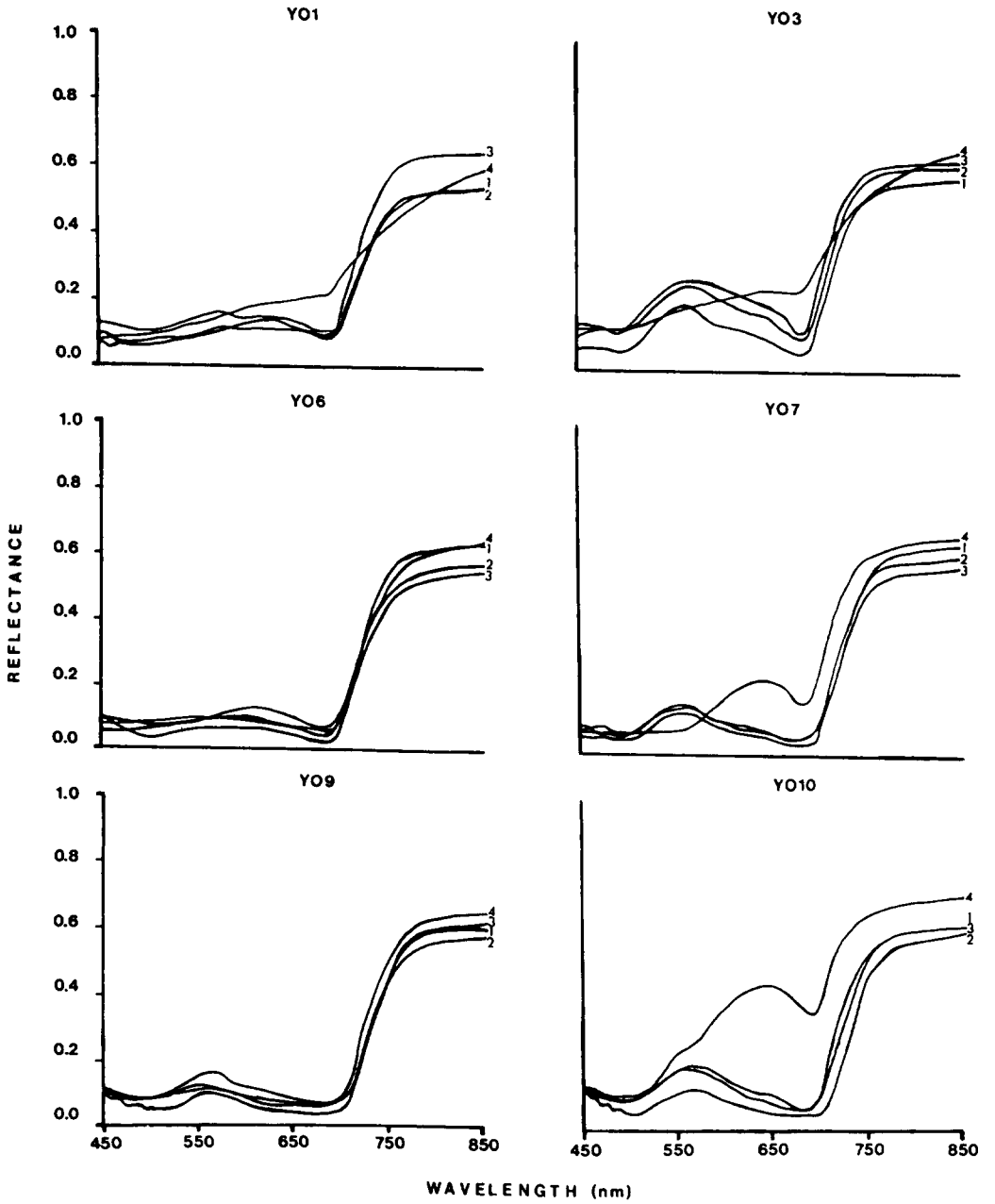

FIGURE 11. Typical reflectance spectra for six trees over four sampling periods. See text for explanation. Sampling dates: 1) 20 Sep.; 2) 24 Sep.; 3) 30 Sep.; 4) 9 Oct.

TABLE 2 Red Shoulder Parameters for Leaves of Pin Oak in Four Stages of Senescence

Tree	Stage	R_s	R_0	R_{sg}	R_{0g}	λ_0	λ_{pg}	σ	λ_{pr}
4	G	0.580	0.068	0.577	0.053	681.6	714.9	33.3	710.9
5	G	0.641	0.036	0.629	0.027	685.5	718.1	32.6	716.4
8	G	0.614	0.043	0.615	0.036	688.2	720.3	32.1	717.5
9	G	0.586	0.062	0.586	0.060	690.7	722.1	31.4	725.3
9	G	0.557	0.034	0.556	0.025	688.0	720.0	32.0	724.2
9	G	0.603	0.057	0.601	0.052	690.0	722.7	32.7	726.4
10	G	0.594	0.043	0.591	0.032	685.8	718.5	32.7	722.0
Mean	G	0.596	0.049	0.594	0.041	687.1	719.5	32.4	720.4
SD	G	0.027	0.013	0.024	0.014	3.106	2.646	0.616	5.652
3	GC	0.565	0.048	0.561	0.012	674.5	707.8	33.3	704.2
3	GC	0.605	0.100	0.601	0.026	671.6	703.5	31.9	704.2
3	GC	0.622	0.110	0.613	0.041	669.2	701.9	32.7	702.0
4	GC	0.656	0.081	0.655	0.047	676.8	709.8	33.0	707.5
4	GC	0.600	0.071	0.595	0.057	678.9	712.7	33.8	706.4
5	GC	0.537	0.057	0.533	0.027	680.0	711.5	31.5	710.9
5	GC	0.573	0.073	0.564	0.068	682.3	716.0	33.7	710.9
7	GC	0.624	0.051	0.621	0.040	683.0	716.0	33.0	709.7
7	GC	0.588	0.046	0.590	0.036	684.2	716.1	31.9	712.0
7	GC	0.552	0.031	0.551	0.007	681.6	714.3	32.7	713.1
8	GC	0.647	0.069	0.646	0.041	679.1	712.0	32.9	709.7
9	GC	0.637	0.065	0.633	0.053	685.4	717.9	32.5	717.5
10	GC	0.617	0.059	0.615	0.020	679.0	711.2	32.2	708.6
10	GC	0.611	0.065	0.608	0.016	676.9	708.3	31.4	707.5
Mean	GC	0.602	0.066	0.599	0.035	678.8	711.4	32.6	708.9
SD	GC	0.036	0.021	0.036	0.018	1.658	4.763	0.753	4.043
1	SE	0.524	0.089	0.518	0.049	672.2	705.7	33.5	704.2
1	SE	0.524	0.074	0.511	0.042	673.9	707.3	33.4	706.4
1	SE	0.634	0.090	0.632	0.045	676.6	709.3	32.7	707.5
4	SE	0.578	0.063	0.564	0.002	669.5	702.3	32.7	702.0
5	SE	0.635	0.180	0.618	0.132	667.8	701.2	34.2	700.9
6	SE	0.614	0.065	0.612	0.037	677.2	710.7	33.5	706.4
6	SE	0.550	0.048	0.545	0.026	680.4	713.4	33.0	709.7
6	SE	0.528	0.029	0.522	0.011	679.9	713.1	33.2	709.7
6	SE	0.617	0.055	0.605	0.048	684.2	716.7	32.5	712.0
8	SE	0.656	0.074	0.649	0.050	676.5	710.3	33.8	704.2
10	SE	0.700	0.341	0.686	0.251	662.0	693.8	31.8	697.5
Mean	SE	0.596	0.101	0.587	0.063	674.6	707.6	33.1	705.5
SD	SE	0.059	0.089	0.059	0.071	6.368	6.555	0.671	4.289
1	SL	0.542	0.237	0.530	0.202	664.5	701.3	36.8	698.6
3	SL	0.617	0.227	0.594	0.189	660.9	707.0	—	702.0
7	SL	0.646	0.149	0.630	0.081	667.7	700.9	33.2	700.9
8	SL	0.582	0.127	0.565	0.090	669.8	704.6	34.8	702.0
Mean	SL	0.597	0.185	0.580	0.141	665.7	703.5	34.9	700.9
SD	SL	0.046	0.055	0.043	0.064	3.885	2.890	1.804	1.603

[1]G = green, GC = green chlorotic, SE = scarlet early, SL: scarlet late. Note: the parameter σ could not be normalized.

1971). The loss of intracellular structure during senescence may also modify spectral response on the red shoulder (Gausman, 1977).

The spectral reflectance from stacked leaves (Fig. 11) when collected over a 4-week period from designated trees (Fig. 8) revealed considerable variation in the stages and intensity of symptoms within and between trees. In many trees symptoms developed slowly, although they were generally consistent with increasing senescence. Tree 6 spectra (Fig. 11, Y06) remained in S_{early} through the sampling period. Anthocyanins, as indicated by the position of the reflectance peak at ± 650 nm, did not increase dramatically through the experimental period. At the same time, chlorophyll degradation was suggested by the change in the R_0 values at ± 700 nm (Table 1). Tree 9 spectra (Fig. 11, Y09) remained green (G) through the experimental period except for sampling period 4, by which time chlorosis had developed (Table 2). Tree 1 (Fig. 11, Y01) was designated S_{early}, throughout with some symptoms of iron chlorosis and weak color development (Treshow, 1970). Trees 7 and 10 (Fig. 11, Y07 and Y010) were also chlorotic at the first sampling but did not have the characteristic dark green vein margins usually associated with iron-induced chlorosis. Tree 10 developed striking red coloration in S_{late} as indicated by the shoulder at ± 640 nm while coloration in Tree 7 was less pronounced. Tree 3 (Fig. 11, Y03) remained in the chlorotic stage through the first three periods but progressed rapidly to S_{late} by the final sampling period (Table 2).

Among the spectral samples, 36 could be assigned unequivocally to four stages of senescence, G, G_c, S_{early}, and S_{late} (Table 2). Remaining categories were insufficient in numbers.

Of the variables studied (Table 2), those discriminating sequentially among symptom classes were the shoulder minimum (R_0), the wavelength corresponding to R_0 (λ_0), and the Gaussian and non-Gaussian inflection points (λ_{pg} and λ_p, respectively). Evidence for a substantial blue shift (Horler et al., 1983) is indicated by the displacement of the mean values for the first derivative maxima from 720.4 to 700.9 nm in the case of the derived data and from 719.5 to 703.5 nm in the Gaussian. Mean values for R_0 increased sequentially from 0.049 to 0.185; at the same time, visual evidence pointed to an accelerated loss of chlorophyll. This did not hold for R_{0g}, however (Table 2).

Values of R_s and R_{sg} did not point to a clear relationship with senescence. The red shoulder parameters (see Methods) from Gaussian data and non-Gaussian

TABLE 3 Percent Success of Red Shoulder Parameters in Identifying Foliar Stages Using a Discriminant Function Analysis

Acronym Senescent Stage	Non-Gaussian	Gaussian	Gaussian and Non-Gaussian
G	85.7	85.7	85.7
G_c	64.3	64.3	71.4
S_{early}	27.3	45.5	45.5
S_{late}	75	100	100
Total misclassified	15/36	12/36	11/36

data were subjected both collectively and separately to a discriminant function analysis (SAS Institute, 1985) after the data distributions were normalized (Table 2). As shown (Table 3), the procedure did not differentiate all categories correctly. As might be expected, late stages of senescence (S_{late}) were discrete, but the difficulty in separating the beginning stages of S_{early} from the later stages of G_c (Table 3) suggests that a more extensive series of symptom categories might have been helpful. Of the three sets of data, combining the Gaussian and non-Gaussian parameters proved most effective with only 11 of 36 samples classified erroneously (Table 3).

Discussion

The progression of senescence in pin oak leaves (*Q. palustris*) can be visualized in terms of three events, each with implications for its spectral reflectance properties. The loss of integrity and disassembly of organelles is a well-marked process (Thomas and Stoddard, 1980); leading in the late phases of senescence to cell "clearing." While not observable in its entirety by light microscopy, it appears to begin with the chloroplasts and ends with the vacuolar membranes (Butler and Simon, 1970) in a well-organized progression of self-lysis (Thomas and Stoddard, 1980). In our studies on pin oak, chloroplast dissolution became evident following, or in conjunction with, anthocyanin development, an observation compatible with the biochemical analyses of Moore (1965) and Sanger (1971). The dissolution of chloroplasts is not the start of the precipitous decline in chlorophyll, an event which other studies clearly show begins some time before senescence is readily discernable (Moore, 1965; Sanger, 1971; Spencer and Titus, 1972). The study by Sanger (1971) might be relevant since it reveals in *Q. ellipsoidalis* an apparent biphasic decline in chlorophyll commensurate with a more rapid disappearance of chlorophyll, presumably as the plastids dissolve. The senescence of chloroplasts in the leaves is sequential (Figs. 2–6), commencing in the upper palisade layer and progressing abaxially to the spongy parenchyma with chloroplasts nearest the substomatal chamber being the last to disappear. This pattern of disassembly may have a significantly different impact on reflectance spectra than a synchronous one.

An important aspect of natural senescence shared with stress-induced senescence is the disappearance of chlorophyll and the development of chlorosis. Spectral detection of stress senescence appears to be closely tied to the loss of chlorophyll (Horler et al., 1983; Goetz et al., 1983).

Anthocyanin and tannin development in leaves is a second well-defined aspect of normal senescence that profoundly affects their reflectance properties. In these studies, anthocyanin development precedes chloroplast disassembly but follows the initiation of chlorophyll degradation, and this is supported by other research (Bogorad, 1958; Moore, 1965; Sanger, 1971). The synthesis of anthocyanins and the causes have been difficult to resolve. The role of light is well known (Bogorad, 1958), but whether anthocyanin synthesis is predicted on increasing or decreasing levels of sugars or shikimic acid seems open to interpretation (Bogorad, 1958; Moore, 1965; Ribereau-Gayon, 1968). The

role of leuco-anthocyanins as colorless precursors of tannins is well established, and the presence of these noncolored precursors may explain some of the uncertainty of the time of origin.

The third event of significance in natural senescence of relevance to spectral change is the alteration of internal geometry as a result of drying. Whereas there are considerable differences between leaves in many anatomical features, leaf drying leads in the R and B stages of senescence to significant changes in cell dimensions relative to leaf dimensions (Table 1).

Many workers have pointed out relationships between key shoulder parameters and physiological or anatomical changes in foliar properties. Enhanced values for R_s associated with losses in chlorophyll have been reported (e.g., Gausman, 1982; Sinclair et al., 1971) and also in experiments where drying and, as a consequence, enhanced light scattering may produce an additive effect on R_s (Gupta and Woolley, 1971; Thomas et al., 1967; 1971). Whereas we did not measure the changes in chlorophyll quantitatively, in both single leaf reflectance measurements (Fig. 10) and in stacked leaves (Fig. 11) there is a perceived rise in R_s related to chlorosis, as deduced from comparisons with the chlorophyll absorption well (R_0) and the green shoulder reflectance maximum at approximately 560 nm. Failure to observe this in the averages of the combined samples (Table 2, R_s and R_{sg}) in spite of directional changes in R_0 and R_{0g} suggests that newly formed anthocyanins and possibly tannins may enhance reflection near the chlorophyll absorption well while dampening reflection on the shoulder (Cardenas et al., 1970). Other factors observed here may also influence reflectance properties particularly the loss of organelles beginning in S_{early} (Figs. 3 and 5).

Not all the physiological and anatomical changes in seasonal senescence may be part of the stress syndrome induced by excess minerals. It is then perhaps significant that there is strong evidence for a blue shift. For oak leaves both λ_{pr} (the observed inflection point) and λ_{pg} (the corresponding Gaussian inflection point) show substantial displacement to shorter wavelengths as senescence progresses (Table 2). That loss of chlorophyll and subsequent chlorosis largely conditions this response (Horler et al., 1983) is supported by the very significant shift that occurs between G and G_c (Table 2) prior to the onset of the major phenomena in senescence that we have discussed.

In conclusion, the interpretation of the events in pin oak leaf senescence as explored anatomically was found to be compatible with the spectral information derived. Key parameters of the red shoulder (Horler et al., 1983) and its Gaussian fit (Hare et al., 1984a,b; Miller et al., 1985) differentiated the senescent stages and were explicable in part on the basis of the anatomical and physiological information available. When a discriminant function analysis was applied to the results, the latter suggest that the use of some Gaussian red-edge parameters permitted better discrimination among the foliar classes than non-Gaussian parameters (Table 3).

This work was supported by a Cooperative Research and Development Grant No. 8451 NSERC. We acknowledge with thanks the expert assistance of Joan M. Boyer in microtechnique.

References

Allen, W. A., Gausman, H. W., Richardson, Q. J., and Cardenas, R. (1971), Water and air changes in grapefruit, corn and cotton leaves with maturation, *Agron. J.* 63:392–394.

Billings, W. D., and Morris, R. J. (1951), Reflection of visible and infrared radiation from leaves of different ecological groups, *Am. J. Bot.* 38:327–331.

Bogorad, L. (1958), The biogenesis of flavanoids, *Ann. Rev. Plant Physiol.* 9:417–448.

Butler, R. D., and Simon, E. W. (1970), Ultrastructural aspects of senescence in plants, *Adv. Gerontol. Res.* 3:73–129.

Canney, F. C., Cannon, H. L., Cathrall, J. B., and Robinson, K. (1979), Autumn colors, insects, plant disease and prospecting, *Econ. Geol.* 74:1673–1676.

Cardenas, R., Gausman, H. W., Allen, W. A., and Schupp, M. (1970). The influence of ammonia-induced cellular discoloration within cotton leaves (*Gossypium hirsutum* L.) on light reflectance, transmittance and absorptance, *Remote Sens. Environ.* 1:199–202.

Collins, N., Chang, S. H., Raines, G., Cassey, F., and Ashley, R. (1983), Airborne biogeochemical mapping of hidden mineral deposits, *Econ. Geol.* 78:737–749.

Gates, D. M., Keegan, H. J., Schleter, J. C., and Weedner, V. R. (1965), Spectral properties of plants, *Appl. Opt.* 4:11–20.

Gausman, H. W. (1977), Reflectance of leaf components, *Remote Sens. Environ.* 6:1–9.

Gausman, H. W. (1982), Visible light reflectance transmittance and absorptance of differently pigmented cotton leaves, *Remote Sens. Environ.* 13:233–238.

Gausman, H. W., Allen, W. A., Myers, V. I., and Cardenas, R. (1967), Reflectance and internal structure of cotton leaves (*Gossypium hirsutum* L.), *Agron. J.* 61:374–376.

Geissman, T. A. (1955), Anthocyanins, chalcones, aurones, flavones and related water soluble pigments in *Modern Methods of Plant Analysis* (K. Paech and M. V. Tracey, Eds.), Springer Verlag, Berlin, pp. 450–498.

Goetz, A. F. H., Rock, B. N., and Rowan, L. C. (1983), Remote sensing for exploration: an overview, *Econ. Geol.* 78:750–760.

Goodwin, T. W. (1958), Studies in carotenogenesis. 24. The changes in carotenoid and chlorophyll pigments in the leaves of deciduous trees during autumn, *Biochem. J.* 68:503–511.

Gupta, R. K., and Woolley, J. T. (1971), Spectral properties of soybean leaves, *Agron. J.* 63:123–126.

Hare, E. W., Miller, J. R., and Edwards, G. R. (1984a), Geobotanical remote sensing of small localized swamps and bogs in Northern Ontario, in *Int. Symp. on Remote Sensing of Environ., Third Thematic Conf., Remote Sensing for Exploration Geology*, Colorado Springs, CO.

Hare, E. W., Miller, J. R., and Edwards, G. R. (1984b), Studies of the vegetation red reflectance edge in eastern Ontario, in *Proc. Ninth Can. Symp. on Remote Sensing*, St. John's, NF, Canada, p. 433.

Horler, D. N. H., Dockray, M., and Barber, J. (1983), The red edge of plant leaf reflectance, *Int. J. Remote Sens.* 4:273–278.

Knipling, E. B. (1969), Leaf reflectance and image formation on color infrared film, in *Remote Sensing in Ecology* (P. L. Johnson, Ed.), Univ. of Georgia Press, Athens, pp. 17–29.

Labovitz, M. L., Masuoka, E. J., Bell, R., Nelson, R. F., Larsen, C. A., Hooker, L. K., and Troensegaard, R. W. (1985), Experimental evidence for spring and autumn windows for the detection of geobotanical anomolies through the remote sensing of

overlying vegetation, *Int. J. Remote Sens.* 6:195–216.

Miller, J. R., Hare, E. W., Neville, R. A., Gauthier, R. P., McColl, W. D., and Till, S. M. (1985), Correlation of metal concentration with anomalies in narrow band multispectral imagery of the vegetation red reflectance edge, in *Int. Symp. on Remote Sensing of Environ., Fourth Thematic Conference, Remote Sensing for Exploration Geology*, San Francisco.

Moore, K. G. (1965), Senescence in leaves of *Acer pseudoplatanus* L. and *Parthenocissus tricuspidata* Planch. 1. Changes in some leaf constituents during maturity and senescence, *Ann. Bot. N. S.* 29:433–444.

Moss, R. A., and Loomis, W. E. (1952), Absorption spectra of leaves. The visible spectrum, *Plant Physiol.* 27:370–391.

Ribereau-Gayon, P. (1968), *Plant Phenolics*, Oliver and Boyd, Edinburgh, 254 pp.

Sanger, J. E. (1971), Quantitative investigations of leaf pigments from their inception in buds through autumn coloration to decomposition in falling leaves, *Ecology* 52:1075–1089.

SAS Institute Inc. (1985), *SAS Users Guide: Statistics*, 5th Ed., SAS, 956 pp.

Sass, J. E. (1951), *Botanical microtechnique*, Iowa State College Press, Ames, 228 pp.

Schwaller, M. R., and Tkach, S. J. (1980), Premature leaf senescence as an indicator in geobotanical prospecting with remote sensing techniques, in *Int. Symp. Remote Sensing of Environment, Proc. 14th Symp.*, San Jose, Costa Rica, pp. 347–358.

Schwaller, M. R., and Tkach, S. J. (1985), Premature leaf senescence as an indicator in geobotanical prospecting with remote sensing techniques, *Econ. Geol.* 80:250–355.

Sinclair, T. R., Hofler, R. M., and Schreiber, M. M. (1971), Reflectance and internal structure of leaves from cereal crops during a growing season, *Agron. J.* 63:864–868.

Spencer, R. W., and Titus, J. S. (1972), Biochemical and enzymatic changes in apple leaf tissue during autumnal senescence, *Plant Physiol.* 49:746–750.

Swain, C. H., and Davis, S. M. (1978), *Remote Sensing: The Qualitative Approach*, McGraw-Hill, New York, 396 pp.

Thimann, K. V. (1980), The senescence of leaves, in *Senescence in Plants* (K. V. Thimann, Ed.), CRC Press, Boca Roton, FL pp. 85–115.

Thomas, H., and Stoddard, J. L. (1980), Leaf senescence, *Ann. Rev. Plant Physiol.* 31:83–111.

Thomas, J. R., Wiegand, C. L., and Myers, V. I. (1967), Reflectance of cotton leaves and its relation to yield, *Agron. J.* 59:551–554.

Thomas, J. R., Nauben, L. N., Oerther, G. F., and Brown, R. G. (1971), Estimating leaf water content by reflectance measurements, *Agron J.* 63:845–847.

Treshow, M. (1970), *Environment and Plant Response*, McGraw-Hill, New York, 422 pp.

Verner, J. E. (1961), Biochemistry of senescence, *Ann. Rev. Plant Physiol.* 12:245–260.

Woolhouse, H. W., and Jenkins, G. I. (1983), Physiological responses, metabolic changes and regulation during leaf senescence, in *The Growth and Functioning of Leaves* (J. E. Dale and F. L. Milthorpe, Eds.), Cambridge Univ. Press, Cambridge, pp. 449–487.

Woolley, J. T. (1971), Reflectance and transmittance of light by leaves, *Plant. Physiol.* 47:656–662.

Received 2 June 1987; revised 3 December 1987.